Phase Division Multiplexed EIT for Enhanced Temporal Resolution

T. Dowrick[1] and D. Holder[1]
[1] Department of Medical Physics & Biomedical Engineering, University College London, UK

Abstract

Objective

The most commonly used EIT paradigm (Time Division Multiplexing) limits the temporal resolution of impedance images due to the need to switch between injection electrodes. Advances have previously been made using Frequency Division Multiplexing (FDM) to increase temporal resolution, but in cases where a fixed range of frequencies is available, such as imaging fast neural activity, an upper limit is placed on the total number of simultaneous injections. The use of Phase Division Multiplexing (PDM) where multiple out of phase signals can be injected at each frequency is investigated to increase temporal resolution.

Approach

TDM, FDM and PDM were compared in head tank experiments, to compare transfer impedance measurements and spatial resolution between the three techniques. A resistor phantom paradigm was established to investigate the imaging of one-off impedance changes, of magnitude 1% and with durations as low as 500µs (similar to those seen in nerve bundles), using both PDM and TDM approaches.

Main results

In head tanks experiments, a strong correlation ($r > 0.85$ and $p < 0.001$) was present between the three sets of measured transfer impedances, and no statistically significant difference was found in reconstructed image quality. PDM was able to image impedance changes down to 500 µs in the phantom experiments, while the minimum duration imaged using TDM was 5 ms.

Significance

PDM offers a possible solution to the imaging of fast moving impedance changes (such as in nerve), where the use of triggering or coherent averaging is not possible. The temporal resolution presents an order of magnitude improvement of the TDM approach, and the approach addresses the limited spatial resolution of FDM by increasing the number of simultaneous EIT injections.

1. Introduction

Electrical Impedance Tomography (EIT) is an imaging technique in which differences in impedance are used to produce an image of the internal structure of an object (Holder 2005), typically by comparing measurements taken at different points in time. Applications of EIT include imaging of lung (Frerichs 2000) and liver (You *et al* 2009), where signals vary in the order of seconds; stroke (Dowrick *et al* 2016), where signals vary over hours/days and evoked potentials (Aristovich *et al* 2016b), where the signals of interest can last for only a few milliseconds. Currently, the imaging of neural signals requires the use of a repeatable, triggered stimulus, and this method has successfully been used to image evoked activity in the rat brain (Aristovich *et al* 2016b).

EIT has been proposed as a method for imaging neural activity inside nerve bundles (Aristovich *et al* 2017), with potential applications in the field of bioelectronic medicine. The ideal paradigm will allow for

real time EIT for imaging of spontaneous activity within nerve bundles, where the duration of an action potential can be as low as 1 millisecond.

Traditional EIT methods are not well suited to this paradigm, as the time taken to collect a full data set is at minimum several milliseconds, which is greater than the event being imaged, which will result in spatial and temporal artifacts. The use of a triggered stimulus is also not possible, as the activity which is to be captured is spontaneous in nature. A solution is presented in this work, using a variation on frequency division multiplexing EIT (FDM-EIT) where in-phase and quadrature components are used at each frequency, to provide additional spatial information in a given frequency range. This approach is referred to as phase division multiplexing EIT (PDM-EIT).

1.1 Limitations of existing EIT approaches

Typical EIT systems inject current in a sequential fashion, which is equivalent to time division multiplexing (TDM). Assuming that voltages are measured in parallel on all electrodes at the same time, the need to switch between electrode pairs imposes a limit on the speed of data acquisition, and therefore the time resolution of the system, which scales with the number of injection pairs used. Theoretically, the minimum time required for data acquisition can be expressed as:

$$n_{inj}/F_c$$

Where n_{inj} is the number of injections and F_c is the injection frequency. This represents the time taken to measure one entire cycle of the input waveform at each injection pair, assuming parallel data recording on all measurement electrodes. In practice, some additional time will required, as more than one period of the injection waveform should be recorded to account for transient effects at the electrodes; there will also be some overhead related to switching between injection pairs and due to the filtering and demodulation applied during signal processing. The time taken can be reduced by either using fewer injection pairs, or by operating at a higher frequency. In the case of nerve activity, the frequency range over which the impedance change is large enough for EIT imaging is 5 kHz-15 kHz. Typical experiments will use a single injection at 9 kHz (Aristovich *et al* 2017), with a bandpass filter of +/-1.5 kHz applied during the signal processing phase of data analysis.

1.2 Principle of FDM/PDM

In this work, an alternative method for imaging short duration events is suggested, using a variant of frequency division multiplexed EIT (FDM-EIT). In FDM-EIT, multiple currents are injected simultaneously, through different electrode pairs, at different frequencies. This approach reduces the time taken to acquire an entire data set, by eliminating the need to switch injection pairs, improving the temporal resolution and allowing for spontaneous activity to be imaged in real time. In this case, the minimum acquisition time is simply $1/F_{min}$, where F_{min} is the lowest injection frequency used. It is possible to inject two signals at each frequency by introducing a phase shift of 90° between them. The two signals will be recorded as a single waveform, but can subsequently be separated as long as the phase of the original signals is known (Figure 1). The two components can be separated by using the Hilbert transform:

$$\phi = angle(H_2/H_1) \quad (1)$$

$$V_{ampl} = abs(H(2)) \quad (2)$$

$$V_{inphase} = \sqrt{(V_{ampl})^2/(1 + tan(\phi_{diff})^2)} \quad (3)$$

$$V_{quadrature} = V_{ampl} \cdot tan(\phi_{diff}) \quad (4)$$

where H_1 denotes the Hilbert transform of the base signal for which the phase is known and H_2 is the Hilbert transform of the measured signal. ϕ is the phase difference between the recorded signal and the original signal at a particular frequency.

Given the usable frequency range of nerve (5 kHz – 15 kHz) and the required signal bandwidth (+/1.5kHz), there are 3-4 usable frequencies. With two injections at each frequency, 6-8 total parallel injections are possible.

1.3 Aims

The aims of this work were:

1. Produce an EIT system which can implement PDM-EIT, as no current EIT system, to the author's knowledge, implements multiple injections, with a quadrature component, over the frequency range of interest.

2. Investigate the use of in-phase and quadrature signals to increase the maximum number of injections when using a limited frequency range.

3. Investigate if there is any statistically significant difference in recorded transfer impedances, and subsequently image quality, when using TDM, FDM and PDM to collect the same data set.

4. Find the maximum temporal resolution of TDM and PDM-EIT, when operating in 'single shot' mode for imaging spontaneous activity.

2. Methods

2.1 Hardware

A typical EIT system will comprise three components, a current source, voltage measurement unit and electrode array, with some capability for routing the injection current to specific pairs of electrodes. In order to meet the requirements of multiple parallel injections, a prototype multi-channel system was created (Figure 2) which comprises multiple identical current sources and an EEG system for simultaneous voltage recording at 100 kHz (ActiChamp - Brain Products GmbH). The circuit used to implement the current source is shown in Figure 3. An ADS9833 DDS chip, programmed over SPI via an Arduino Nano, was used for sine wave generation, which allows control of both the frequency and phase of each output signal. A single master clock was used to synchronise all DDS chips, allowing for a constant phase delay to be introduced between pairs of signals to produce the in-phase and quadrature components. A decoupling capacitor on the AD9833 output line centres the waveform around 0V, with adjustable gain provided by the non-inverting amplifier constructed with op-amp A. The voltage waveform was converted to a double ended signal, using op-amps B and C and a differential Howland current pump, op-amps D and E, used to perform V-I conversion. The differential current pump was used in place of the 'standard' HCP, to prevent interference between different injection currents. Lithium Polymer batteries provided +/- 3 V supply lines, RC4560 dual package op-amps were and 0.1% tolerance resistors were used. Circuit schematics, PCB layouts and source code to replicate the multi-channel current source are available under an open source license (https://github.com/EIT-team/Parallel-CS).

2.2 Tank study

An important aspect to compare between TDM, FDM and PDM was whether the different data collection and processing methods introduce any differences in measured transfer impedances, when collecting data

in the same situation e.g. using an equal number of impedance measurements and an equal amount of data averaging.. In order to make this comparison of data, and subsequently image quality, tank experiments were carried out using a 32 electrode neonatal head tank (Avery *et al* 2017a), diameter 13cm, including realistic skull with fontanelles (Figure 4), filled with 0.1% concentration saline.

The three methods compared were TDM using 4 sequential injections pairs (ScouseTom EIT system (Avery *et al* 2017b)) at 4 kHz, FDM using 4 different frequencies (1 kHz, 2 kHz, 3 kHz, 4 kHz) and PDM with the use of in-phase and quadrature components at two frequencies (2 kHz, 4 kHz). The injection currents were 100 μA in amplitude in all cases. A plastic ball, 2 cm in diameter (15% of the total tank diameter), was introduced as a perturbation in the tank at 4 positions (anterior, posterior, lateral, central), positioned with 5 mm accuracy. For each method and for each position, a baseline dataset was collected, followed by an additional dataset once the perturbation has been introduced. Data was recorded for 100 ms in each case.

4 injection pairs were used for data recording. The choice of injection pairs was decided by simulation, to identify injections which maximized sensitivity throughout the skull. In practice, this results in injections which maximise the distance between the two electrodes and that are aligned with the fontanelles in the skull. Voltages were recorded at all electrodes, but any electrodes which were used for current injection were removed from the final data set. In the case of PDM and FDM, this results in 96 transfer impedance measurements, as 8 electrodes were used simultaneously for injection. In order to allow for a like-for-like comparison of data, the same 96 measurements were extracted from the TDM data set.

1.3 Data processing

A 5th order Butterworth filter, with a bandwidth of 500 Hz was applied around each carrier frequency, after which the amplitude of the signal was extracted using the Hilbert transform. For the PDM data set, the in-phase and quadrature components were separated using the (Figure 1, equations (1) – (4)).]The mean amplitude, over 100 cycles of the injected current, was calculated for the baseline and perturbation periods, to produce one set of voltage difference data for each perturbation. Manual inspection of the voltage data was undertaken to remove erroneous data points - measurements which exhibited noise greater than 0.1mV were removed. Image reconstructions used a 0th order Tikhonov algorithm and noise based correction (Dowrick *et al* 2016), with a 200,000 element mesh for the head tank. The noise based correction assigns each element in the mesh a value according to the significance of the change, rather than an absolute impedance value. Images were rendered using ParaView, with a full-width half-max threshold applied. The quality of the reconstructed image was assessed using three image quantification metrics(Malone *et al* 2014):

- Localisation error: the displacement of the centre of mass of the reconstructed perturbation with respect to its real position, as a percentage of the tank's diameter.
- Shape error: the mean of the difference in each axis of the reconstructed perturbation to the perturbation's actual width, expressed as a percentage of the tank's diameter.
- Image noise: the standard deviation of all conductivity changes not belonging to the reconstructed perturbation, expressed as a percentage of the mean of the reconstructed perturbation's conductivity changes.

2.4 Temporal resolution measurements in resistor phantom

The intended application of PDM-EIT is to allow for EIT data to be collected of spontaneous, one-off activity in peripheral nerves, with millisecond durations, where the use of triggered stimulus and repeated averaging over time is not possible (Aim 4) and where the usable frequency range is limited. In this

scenario, the goal of the EIT imaging is to accurately locate the region in which activity is occurring and the duration of activity. In order to evaluate the method, an additional set of experiments was devised to compare the ability of PDM and TDM to image millisecond impedance changes in a resistor phantom. A 32 electrode resistor phantom, comprising 96 resistors with values between 330 Ω and 1 kΩ resistors (the resistance between two adjacent electrodes was 2.7 kΩ), which approximates a cylindrical object, was used.

The experiment was designed to mimic the situation in nerve, where separate bundles of activity occupy different regions of the nerve cross section. In this case, the phantom was considered to have four distinct quadrants (between electrodes 1-8, 9-16, 17-24, 25-32) in which activity could occur, and a small (+1%) resistance change, with arbitrary duration, was introduced into each quadrant of the phantom. The resistance change was introduced into the phantom using an additional digital switching circuit (ADG714), to switch An additional circuit, used a digitally controlled ADG714 switch to introduce a single additional resistor (30 Ω/1%) into a given quadrant of the phantom. The switching/settling time of the ADG714 itself is in the order of 10 ns, which can be considered negligible. Additional methods for assessing the temporal resolution of the system were considered, including tank based experiments, but none were able to offer the same level of control over the magnitude and duration of changes.

Two pass/fail criteria were established to assess success. First, the duration of the reconstructed impedance change should match the real value, which is set in the control software. Second, the centre of mass of the impedance change should be located within the correct quadrant of the mesh.

Two sets of data were collected. In the first, resistance changes with durations of 10 ms, 5 ms, 2 ms, 1 ms or 0.5 ms were generated sequentially in each quadrant of the phantom over a 1 second period. No triggering was used and each impedance change was introduced only once. To emulate a scenario more comparable to the intended application in nerves, a second data set was collected, where a sequence of 8 impedance changes, with randomly assigned duration (0.5 ms to 2.5 ms) and position were generated over a one second period.

All experiments were repeated for TDM-EIT with 4 sequential current injection pairs at 5.5 kHz, and for PDM-EIT with 4 simultaneous injections (in-phase and quadrature at both 4 kHz and 5.5 kHz). The exact frequencies chosen do not affect the operation of the PDM-EIT system in phantom/tank experiments, where the impedance spectrum is constant. For the intended applications in nerve imaging, the frequencies at which the impedance changes in the tissue are at a maximum are known to be between 5 kHz and 15 kHz, and frequencies in this range would be selected. Injection currents of amplitude 100μA were used in all cases. For TDM-EIT, in order to allow sufficient cycles of the waveform to be captured to account for electrode settling and signal processing overheads, the injection time for each injection pair was set to 1 ms (5 cycles of the waveform), for a total data collection time of 4 ms. Voltages were recorded at all 32 electrodes; resulting in 120 transfer impedance measurements for TDM-EIT and 96 for PDM-EIT, once the voltages at the injection electrodes had been discarded.

2.5 Data processing

The same filtering and demodulation steps was carried out as for the tank experiments, but with an increased filter bandwidth of +/- 1.5 kHz, to reflect the higher frequency impedance changes being recorded. For each PDM-EIT data set, with duration one second, data was split into 0.5 ms segments, which is equivalent to 2 cycles of the 4kHz signals and 2.75 cycles of the 5.5 kHz signals. Data was averaged within each segment, and the first segment was taken as the baseline. Voltage difference data was calculated for each subsequent segment (199 total dV measurements). TDM-EIT data was split in 4ms segments, equal to the time required for a single set of measurements. The same data rejection criteria as for the tank study was employed, where data points with noise greater than 0.1 mV were

rejected. A 20,000 element cylindrical mesh was used for image reconstruction, and images were again rendered using ParaView.

3. Results

3.1 Tank experiments

The average number of transfer impedance measurements excluded from each set of 96 was 1 (min = 0, max = 4).In the voltage difference data (Figure 5), a strong correlation ($r > 0.85$ and $p < 0.001$) was present between the three sets of measured data. For each of the four locations in which the perturbation was placed, the location and shape error, generated from the reconstructed images (Figure 6) were below 4% and the noise error below 5% (Table 1, Figure 7). p-values greater than 0.85 were calculated using 1-way ANOVA, indicating that there was no statistically significant difference between the three sets of images.

Table 1 - Mean image quantification errors, across the 4 perturbation locations, for each of the measurement techniques. No significant difference was present between any of the data sets ($p > 0.85$ using 1-way ANOVA).

	Location error	Shape error	Noise error	Total error
TDM	3.0%	3.0%	4.4%	10.5%
FDM	2.9%	2.9%	4.1%	9.9%
PDM	2.7%	2.7%	3.9%	9.5%

3.2 Temporal resolution

An average of 1 (min = 0, max = 4) transfer impedance measurements, out of 96, 4 transfer impedance measurements were excluded from the final data TDM/PDM data sets, due to excessive noise. When using the PDM-EIT system to image impedance changes of 10 ms, 5 ms, 2 ms, 1 ms and 0.5 ms, it was possible to image the location and duration of each impedance change (Figure 8) across all measurements, in line with the success/failure criteria set out. The shortest impedance change that could be imaged using TDM-EIT was 10 ms. It was also possible to image all changes during the randomly generated sequence of impedance changes using PDM-EIT. Voltage difference of ~5 μV were exhibited in response to each impedance change (Figure 9), which matches the 1% impedance change introduced into the circuit. See accompanying video for the image reconstructions. TDM-EIT was unsuccessful in reconstructions in all instances.

4. Discussion

TDM, FDM and PDM EIT, using the same number of injections were compared in a head tank, imaging a static plastic perturbation in four positions. No significant difference between measured transfer impedances (correlation $r > 0.85$, $p < 0.001$) or image accuracy was detected in the reconstructed images,

with the mean error for all cases within the margin of error involved with repeatedly placing the perturbation in the same location, which has a margin of error of 5 mm. These results demonstrate that there is no additional error introduced into the reconstruction process due to the additional data collection and processing requirements for PDM-EIT.

The use of simultaneous, EIT injections at different frequencies, to image impedance changes of 1%, with durations as small as 500 μs has been demonstrated. This is more than an order of magnitude improvement when compared to the use of TDM-EIT, which could only successfully image 10ms changes, and is comparable to the time scale associated with neural signals. While the 4ms data collection time for TDM-EIT should in theory allow for imaging 5 ms impedance changes, unless the impedance change is synchronized to the start of a measurement cycle, the impedance change will take place over two separate measurement frames, resulting in significant error. Additionally, it has been shown that multiple signals can be injected at the same frequency, overcoming one of the limitations associated with standard frequency division multiplexing approaches, for applications where the usable frequency range is limited.

While the feasibility of PDM-EIT has been demonstrated here, the authors acknowledge that further work is needed to apply this new technique to ex-vivo and in-vivo models. Previous work to image in nerve using TDM (Aristovich *et al* 2016a) indicates that relevant activity may occupy 10-20% of the nerve diameter, in a 2D cross section, equal to 1-5% of the total area. In the 3D head tank experiments, a 2 cm perturbation, equivalent to 15% of the tank diameter and occupying ~1% of the total volume, was imaged using 4 current injection pairs. While not directly comparable, due to the different imaging methods, this does suggest there is sufficient spatial accuracy, even considering the reduced number of current injections available using PDM. There are, however, a number of additional challenges which need to be considered for in-vivo use of FDM/PDM-EIT. First, the hardware used must be sufficiently low noise, to provide a sufficient SNR for imaging. Secondly, any variations in the impedance response of the tissue at different frequencies should be known and accounted for. Thirdly, in order to successfully use in-phase and quadrature waveforms at the same frequency, the phase delay introduced by the nerve itself must be either negligible, or also accounted for.

References

Aristovich K, Blochet C, Avery J, Donega M and Holder D 2016a EIT of evoked and spontaneous activity in peripheral nerve *17 th International Conference on Electrical Impedance Tomography*

Aristovich K, Donega M, Perkins J, Fjordbakk C, Avery J and Holder D 2017 stIn-vivo EIT imaging of spontaneous phasic activity in peripheral nerves *Proceedings of the 18th International Conference on Biomedical Applications of Electrical Impedance Tomography* p 37

Aristovich K Y, Packham B C, Koo H, Santos G S Dos, McEvoy A and Holder D S 2016b Imaging fast electrical activity in the brain with electrical impedance tomography. *Neuroimage* **124** 204–13 Online: http://www.sciencedirect.com/science/article/pii/S1053811915007922

Avery J, Aristovich K, Low B and Holder D 2017a Reproducible 3D printed head tanks for electrical impedance tomography with realistic shape and conductivity distribution *Physiol. Meas.* **38** 1116–31

Avery J, Dowrick T, Faulkner M, Goren N and Holder D 2017b A Versatile and Reproducible Multi-Frequency Electrical Impedance Tomography System *Sensors* **17**

Dowrick T, Blochet C and Holder D 2016 In vivo bioimpedance changes during haemorrhagic and ischaemic stroke in rats: towards 3D stroke imaging using electrical impedance tomography *Physiol. Meas.* **37** 765 Online: http://stacks.iop.org/0967-3334/37/i=6/a=765

Frerichs I 2000 Electrical impedance tomography (EIT) in applications related to lung and ventilation: a review of experimental and clinical activities *Physiol. Meas.* **21** R1–21 Online: http://www.scopus.com/inward/record.url?eid=2-s2.0-0034039948&partnerID=tZOtx3y1

Holder D S 2005 *Electrical impedance tomography: methods, history, and applications* (Institute of Physics Publishing) Online: http://books.google.com/books?id=cjcRd4m_jUQC&pgis=1.

Malone E, Jehl M, Arridge S, Betcke T and Holder D 2014 Stroke type differentiation using spectrally constrained multifrequency EIT: Evaluation of feasibility in a realistic head model *Physiol. Meas.* **35** 1051–66

You F, Shuai W, Shi X, Fu F, Liu R and Dong X 2009 In vivo monitoring by EIT for the pig's bleeding after liver injury *IFMBE Proceedings* vol 25 pp 110–2 Online: http://www.scopus.com/inward/record.url?eid=2-s2.0-77950909455&partnerID=tZOtx3y1

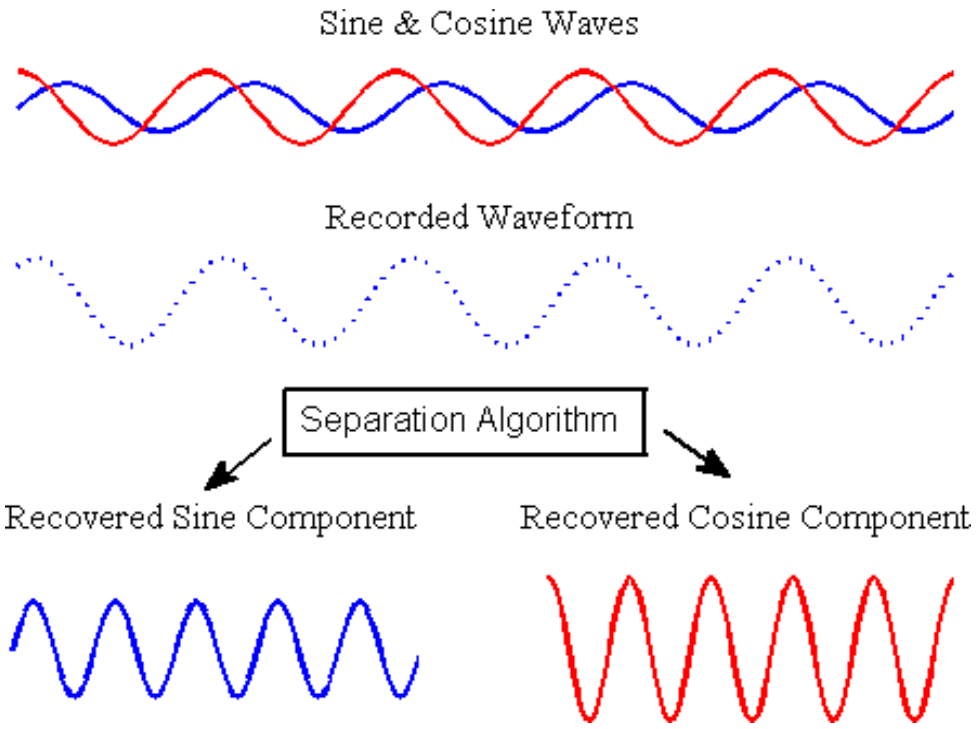

Figure 1 - Two signals, injected 90 degrees out of phase, can be separated after recording, by utilsing knowledge of the original phase relationship.

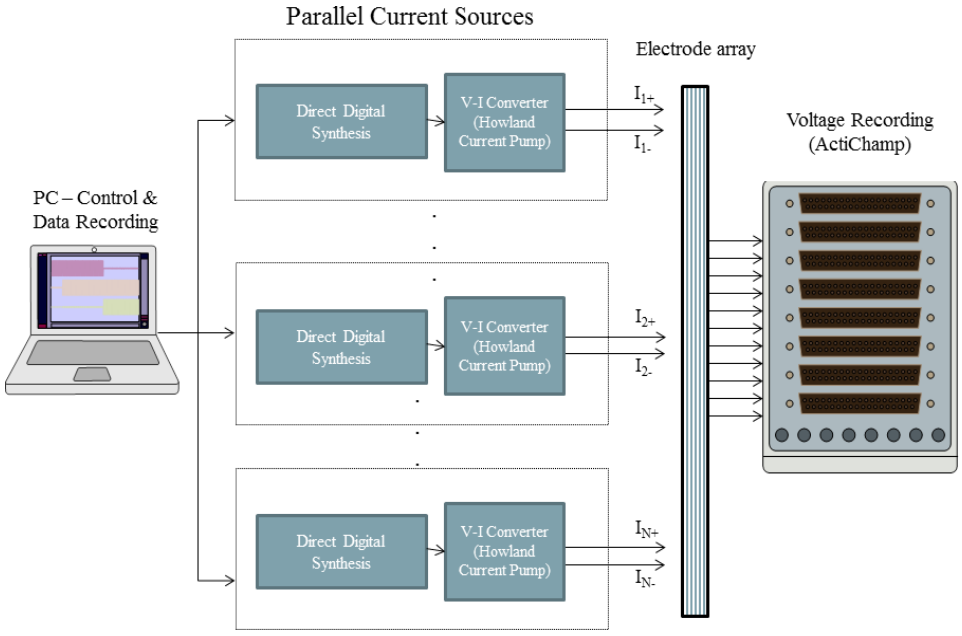

Figure 2 - Block diagram of PDM-EIT system. Multiple independently programmed current sources inject in parallel across the electrode array. Voltage measurements are taken at all electrodes simultaneously using the actiCHamp EEG system. A host PC interfaces with the current sources and controls the measurement process.

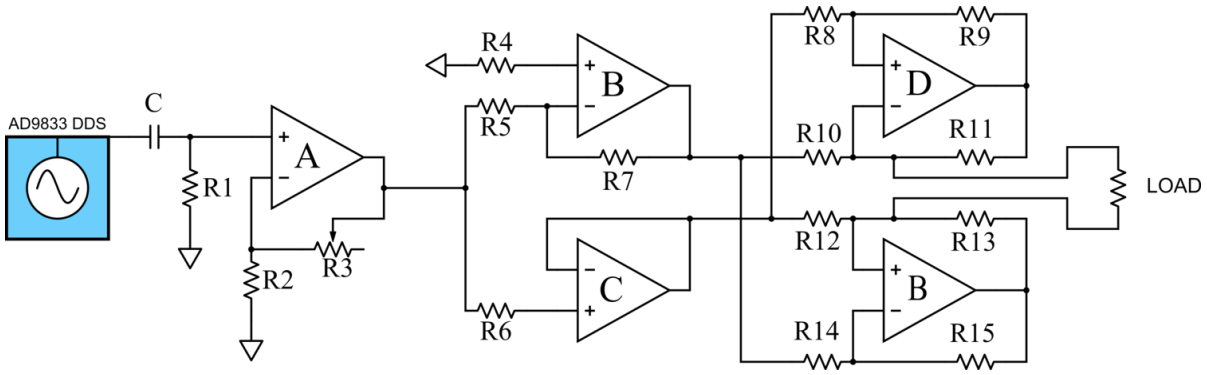

Figure 3 - Circuit used to implement voltage to current conversion. The decoupling capacitor centres the DDS output voltage around 0 V. Op amp A provides adjustable gain, op amps B and C converts the single ended voltage signal to a differential signal, and op amps D and E implement a differential Howland Current Pump.

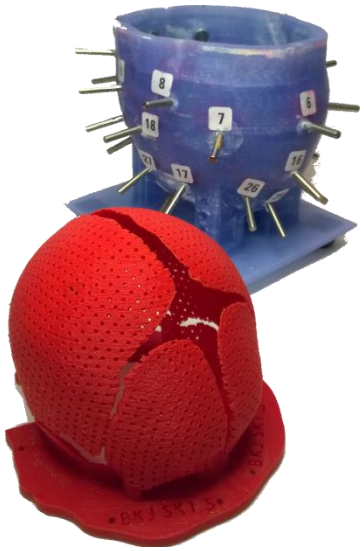

Figure 4 - 32 Channel neonatal head tank.

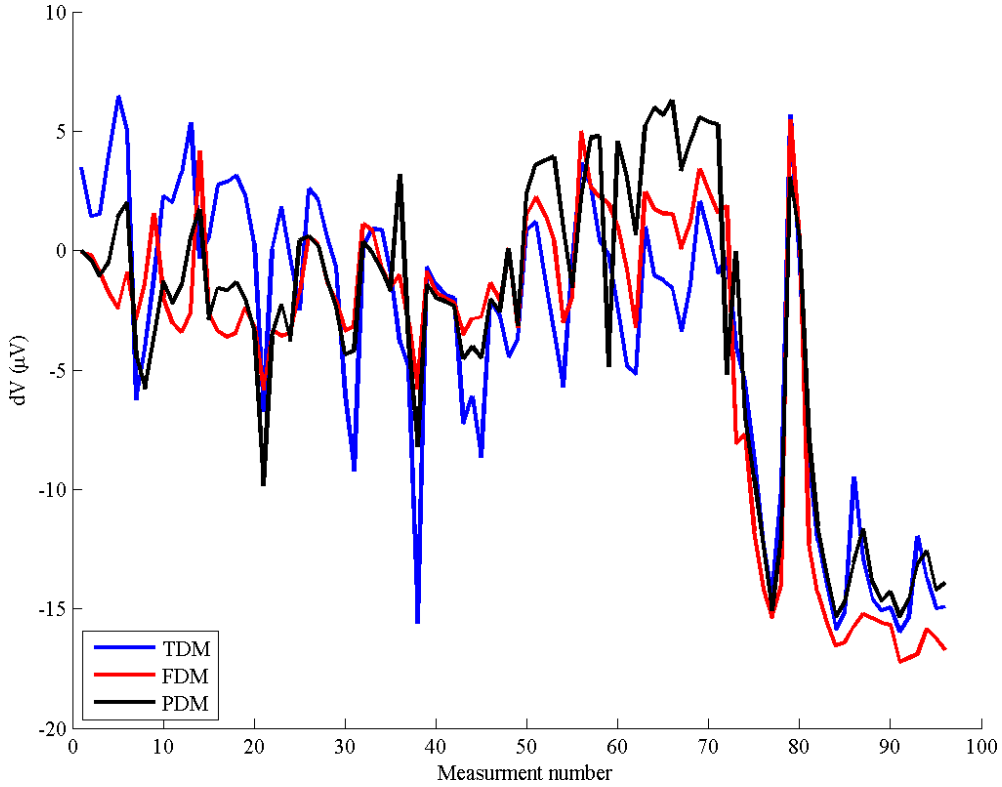

Figure 5 - Single set of voltage difference data, for each of the three measurement methods. $r > 0.85$ and $p < 0.001$ for all combinations of data sets.

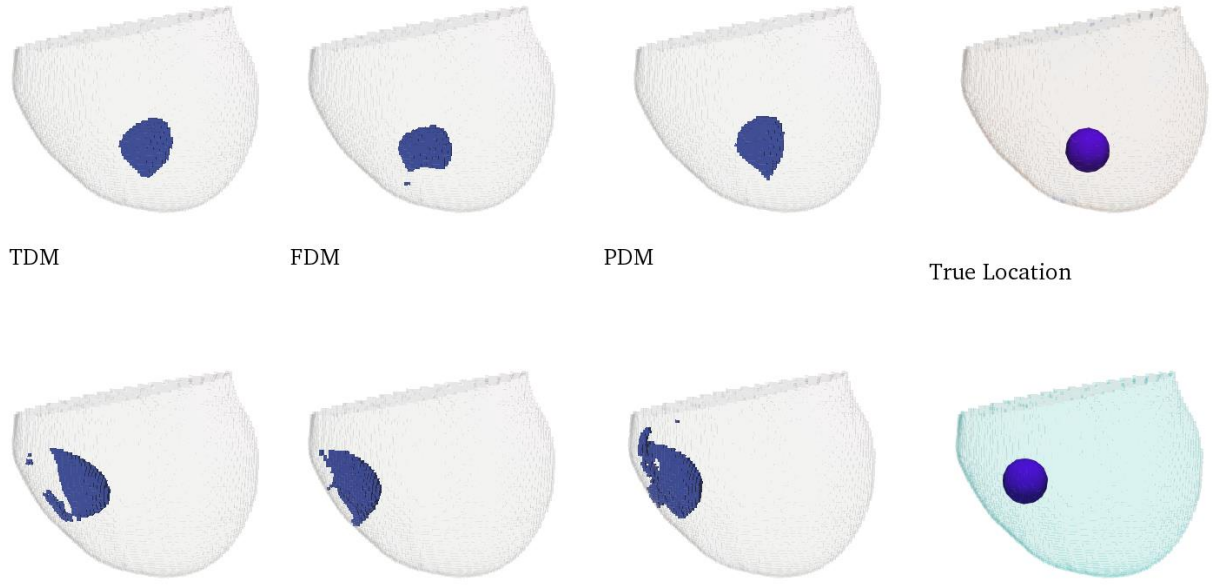

Figure 6 - Image reconstructions in neonate tank. Two different perturbation positions are shown, for the TDM, FDM and PDM cases, along with the true position of the perturbation.

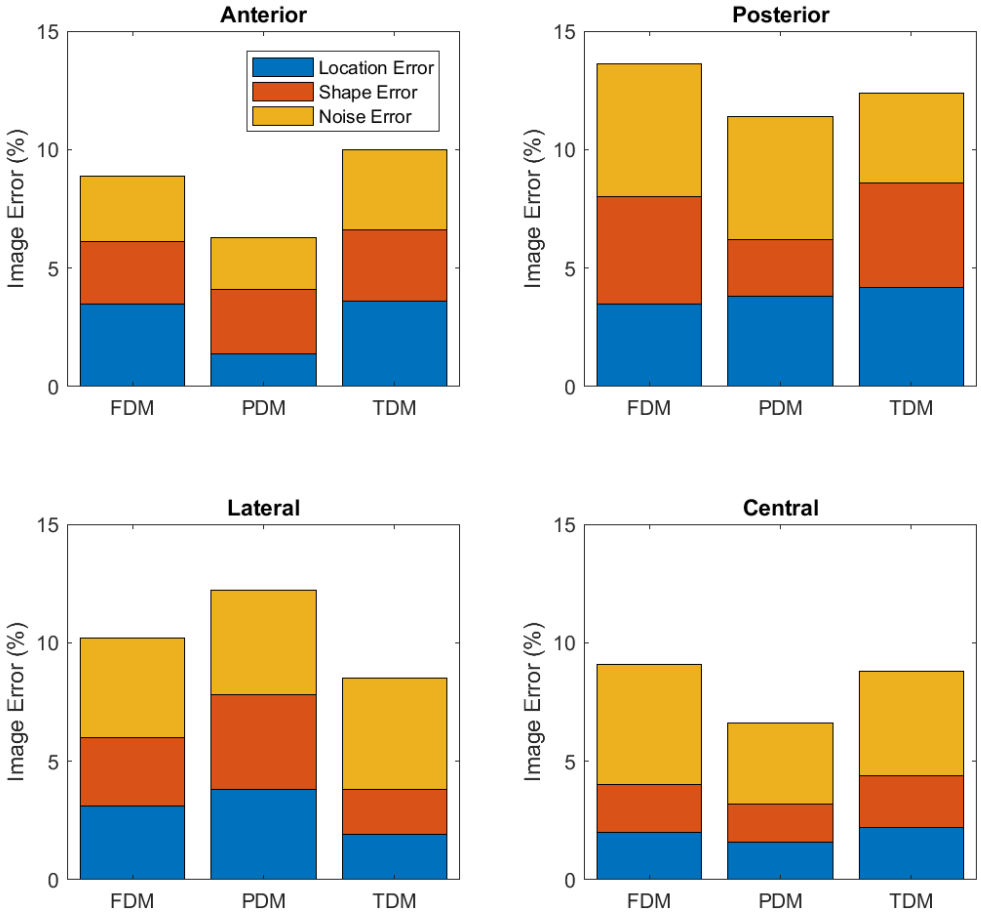

Figure 7 - Image error for TDM, FDM and PDM in four locations. Difference between the different techniques were not found to be statistically significant ($p > 0.85$ using 1-way ANOVA).

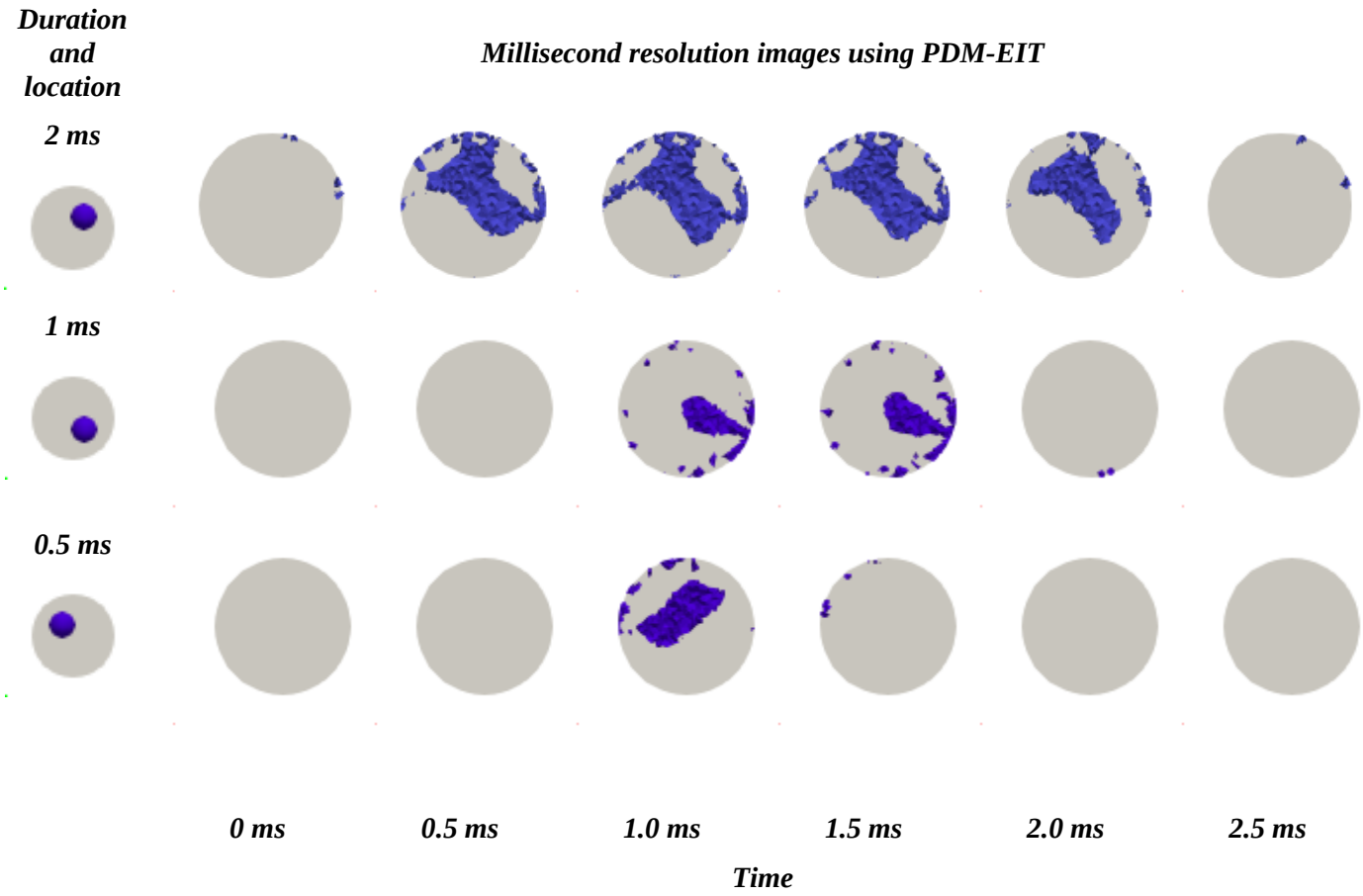

Figure 8 – Sample of image reconstructions using PDM-EIT data collected on resistor phantom, with impedance changes of duration 2 ms, 1 ms and 0.5 ms. The location and duration of the impedance change is given in the leftmost column, and was successfully replicated in the image reconstructions.

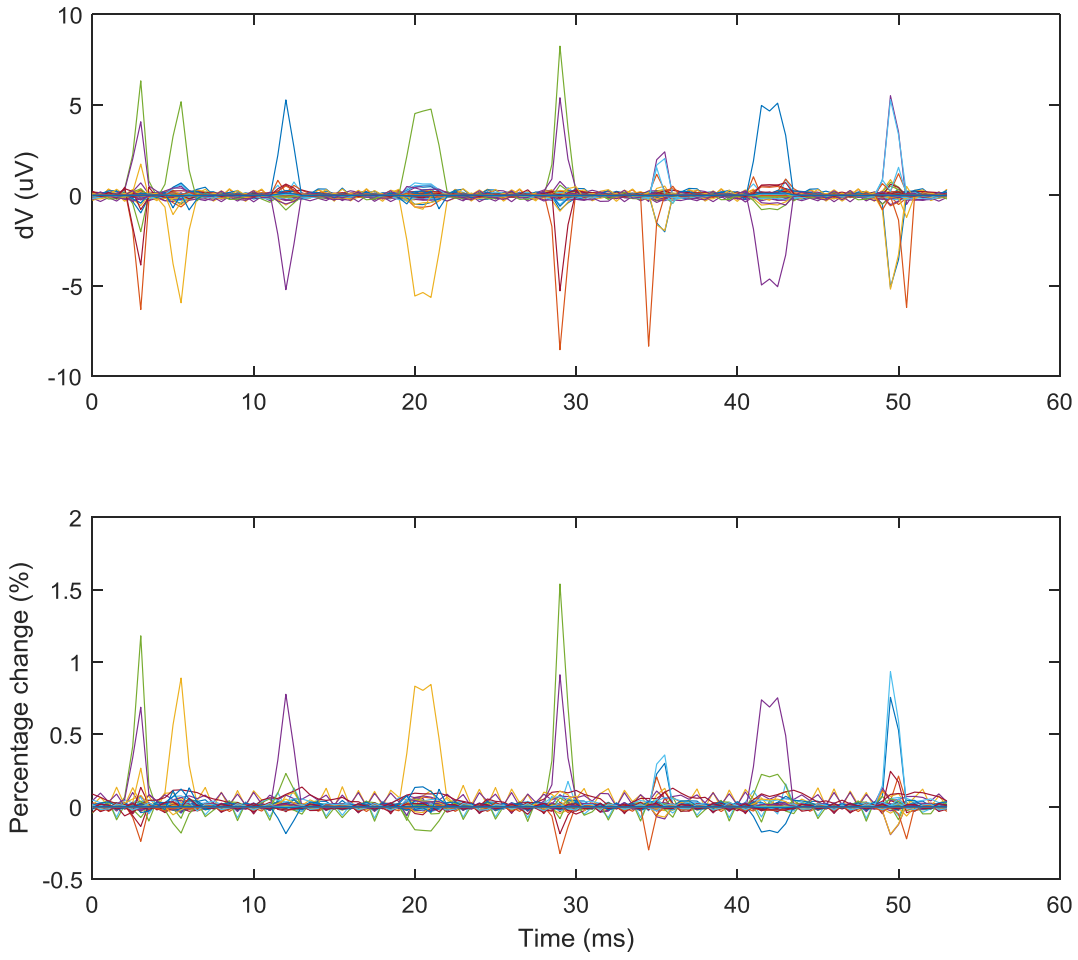

Figure 9 - Voltage difference data for a sequence of 8 impedance changes, with durations 0.5 ms to 2.5 ms, introduced into the resistor phantom. The expected impedance change is in the order of 1%. Image reconstructions are shown in the video attached to this paper.